Study of natural diversity in response to a key pathogenicity regulator of Ralstonia solanacearum reveals new susceptibility genes in Arabidopsis thaliana

Choghag Demirjian, Narjes Razavi, Henri Desaint, Fabien Lonjon, Stéphane Genin, Fabrice Roux, Richard Berthomé, Fabienne Vailleau

HAL Id: hal-03621760

https://hal.inrae.fr/hal-03621760v1

Submitted on 28 Mar 2022

ORIGINAL ARTICLE

Study of natural diversity in response to a key pathogenicity regulator of *Ralstonia solanacearum* reveals new susceptibility genes in *Arabidopsis thaliana*

Choghag Demirjian[1] | Narjes Razavi[1] | Henri Desaint[1,2] | Fabien Lonjon[1] |
Stéphane Genin[1] | Fabrice Roux[1] 🆔 | Richard Berthomé[1] | Fabienne Vailleau[1] 🆔

[1]LIPME, Université de Toulouse, INRAE, CNRS, Castanet-Tolosan, France

[2]SYNGENTA Seeds, Sarrians, France

Correspondence
Fabienne Vailleau, LIPME, Université de Toulouse, INRAE, CNRS, Castanet-Tolosan, France.
Email: fabienne.vailleau@inrae.fr

Present address
Fabien Lonjon, Department of Cell & Systems Biology, University of Toronto, Toronto, Ontario, Canada

Funding information
Grant/Award, Grant/Award Number: Campus France, French Ministry of National Education and Research, Lebanese University and Syngenta seeds; INRAE Plant Health and Environment division; Occitanie Regional Council

Abstract

Ralstonia solanacearum gram-negative phytopathogenic bacterium exerts its virulence through a type III secretion system (T3SS) that translocates type III effectors (T3Es) directly into the host cells. T3E secretion is finely controlled at the posttranslational level by helper proteins, T3SS control proteins, and type III chaperones. The HpaP protein, one of the type III secretion substrate specificity switch (T3S4) proteins, was previously highlighted as a virulence factor on *Arabidopsis thaliana* Col-0 accession. In this study, we set up a genome-wide association analysis to explore the natural diversity of response to the *hpaP* mutant of two *A. thaliana* mapping populations: a worldwide collection and a local population. Quantitative genetic variation revealed different genetic architectures in both mapping populations, with a global delayed response to the *hpaP* mutant compared to the GMI1000 wild-type strain. We have identified several quantitative trait loci (QTLs) associated with the *hpaP* mutant in-oculation. The genes underlying these QTLs are involved in different and specific biological processes, some of which were demonstrated important for *R. solanacearum* virulence. We focused our study on four candidate genes, *RKL1*, *IRE3*, *RACK1B*, and *PEX3*, identified using the worldwide collection, and validated three of them as susceptibility factors. Our findings demonstrate that the study of the natural diversity of plant response to a *R. solanacearum* mutant in a key regulator of virulence is an original and powerful strategy to identify genes directly or indirectly targeted by the pathogen.

KEYWORDS
Arabidopsis thaliana, GWA mapping, HpaP T3S4 protein, natural accessions, *Ralstonia solanacearum*, susceptibility genes

1 | INTRODUCTION

In nature, plants are constantly challenged by pathogen attacks. However, due to efficient innate immune responses induced by the multilayered defence strategies deployed by plants, disease rarely occurs. The first layer of plant defence takes place via the perception of conserved pathogen-associated molecular patterns (PAMPs) through host cell surface pattern recognition receptors (PRRs), which activate pattern-triggered immunity (PTI) (Bigeard et al., 2015). Successful pathogens counteract PTI by injecting directly into the host cells virulence factors, called effectors, resulting in effector-triggered susceptibility (ETS). The recognition of these pathogen effectors through plant nucleotide-binding domain, leucine-rich repeat (NLR) immune receptors activates a second layer of a pathogen- and strain-specific plant defence response called effector-triggered immunity (ETI) (Cesari, 2018; Jones & Dangl, 2006). ETI is generally associated with a programmed cell death referred to as a hypersensitive response (HR). Another form of resistance that is predominant in crop and wild species corresponds to quantitative disease resistance (QDR) (Roux et al., 2014). Based on a polygenetic determinism, QDR is more durable than ETI in crop fields by providing a reduction rather than an absence of disease. In addition, QDR generally confers broad-spectrum resistance (Roux et al., 2014).

Ralstonia solanacearum, the causal agent of bacterial wilt, is one of the most important bacterial diseases worldwide. This soilborne pathogen attacks more than 200 plant species, including many important crops (Hayward, 1991) and the model wild plant *Arabidopsis thaliana* (Deslandes et al., 1998). The main determinant of *R. solanacearum* pathogenicity consists of a type III secretion system (T3SS), a true "molecular syringe", that allows the translocation of a large arsenal of type III effectors (T3Es) directly into the host cell (Sabbagh et al., 2019). These T3Es promote bacterial virulence by subverting plant innate immunity and modifying host metabolism (Landry et al., 2020). The transcriptional regulatory network of *R. solanacearum* type III secretion (T3S) is very well described in the literature (Coll & Valls, 2013). In addition, increasing information is available concerning the function of type III-associated regulators at the posttranslational level, such as type III chaperones (T3Cs) and type III secretion substrate specificity switch (T3S4) proteins (Lohou et al., 2013). Recent studies showed that *R. solanacearum* Hpa (for "hypersensitive response and pathogenicity-associated") proteins interact with T3Es (Lohou et al., 2014; Lonjon et al., 2017) and regulate T3E secretion (Lonjon et al., 2016, 2020). However, the precise role of these helper proteins in *R. solanacearum* virulence is not fully understood yet. For instance, the *hpaB* mutant is strongly altered in its T3S and HpaB is strictly required for *R. solanacearum* pathogenicity on *A. thaliana*, *Medicago truncatula* (Lonjon et al., 2016), and tomato plants (Lonjon et al., 2017). HpaG, a negative regulator of T3S, is specifically required for *R. solanacearum* full pathogenicity on *M. truncatula* (Lonjon et al., 2016). Although an *hpaP* mutant is little affected on its T3S (Lonjon et al., 2020), the HpaP T3S4 protein is an important virulence factor of *R. solanacearum* on both *A. thaliana* and tomato plants (Lohou et al., 2014). This finding differs from previous literature where 54 *R. solanacearum* single T3E

mutants were not affected in their virulence on susceptible *A. thaliana* and tomato plants (Cunnac et al., 2004). Hence, the HpaP example illustrates the importance of studying the role of these helper proteins in disease promotion. Therefore, functional characterization of *R. solanacearum* T3Es, and also of these Hpa proteins and of their plant targets, could be pivotal to identify components of plant immunity.

To date, no durable strategy to protect plants against bacterial wilt is available, and the use of resistant or tolerant cultivars appears to be the best disease control strategy (Huet, 2014). In *A. thaliana*, several genetic loci conferring resistance to *R. solanacearum* have been identified through the phenotyping of recombinant inbred line populations (Peeters et al., 2013). First identified in Nd-1 accession, the *RRS1-R* gene, encoding a Toll/interleukin-1 receptor-nucleotide-binding site leucine-rich repeat (TIR-NBS-LRR) protein with a WRKY C-terminal domain, confers resistance against the GMI1000 *R. solanacearum* strain through the direct recognition of the PopP2 T3E (Deslandes et al., 2002, 2003). This resistance was further demonstrated to function via the RPS4/RRS1-R pair of immune receptors (Le Roux et al., 2015). The *ERECTA* gene, encoding an LRR receptor-like kinase (LRR-RLK), was identified as a QDR gene to the 14.25 *R. solanacearum* strain in Col-0 accession (Godiard et al., 2003). These studies revealed the potential of exploiting the genetic diversity of *A. thaliana* to set up quantitative genetic studies. Accordingly, using the *R. solanacearum* GM1000 wild-type strain, genome-wide association studies (GWAS) performed on a worldwide collection of *A. thaliana* not only confirmed the *RPS4/RRS1-R* locus as the main quantitative trait loci (QTLs) of resistance to GMI1000 at 27°C, but also revealed *AtSSL4*, which encodes a strictosidine synthase-like protein, as a susceptibility gene at 30°C (Aoun et al., 2017). Another GWAS based on the highly genetically diverse local population TOU-A (population A from Toulon-sur-Arroux, France; Frachon et al., 2017) identified another QDR gene to GMI1000 at 30°C, that is, the atypical meiotic cyclin *SOLO DANCERS* gene (Aoun et al., 2020). More recently, a GWAS using an in vitro system allowing the study of *A. thaliana* early root phenotypes after *R. solanacearum* inoculation highlighted a new role for cytokinin in root immunity in response to GMI1000 (Alonso-Díaz et al., 2021). Altogether, these results confirmed the benefit of considering different mapping populations in GWAS to unravel the genetics of complex quantitative traits (Bergelson & Roux, 2010; Brachi et al., 2013).

In this study, to better understand the role of the HpaP T3S4 protein, we aimed to identify the plant factors potentially controlled by *R. solanacearum* in an HpaP-dependent manner. For this purpose, we set up a GWAS on the natural diversity of response to the *hpaP* mutant in both worldwide and local mapping populations of *A. thaliana*. Interestingly, the extent of genetic variation for QDR and the underlying genetic architecture largely differed between GMI1000 wild-type strain and *hpaP* mutant as well as between the two mapping populations. In addition, the *hpaP* response was associated with original biological processes. We then focused our study on four candidate genes underlying QTLs and analysed their expression patterns in selected resistant and susceptible worldwide accessions to the *hpaP* mutant. A reverse genetic approach highlighted the three genes *RKL1*, *RACK1B*, and *PEX3* as involved in plant susceptibility to bacterial wilt.

2 | RESULTS

2.1 | Quantitative genetic variation reveals contrasting responses to *R. solanacearum hpaP* mutant in two complementary mapping populations

In this study, we used two *A. thaliana* mapping populations, a worldwide collection (176 accessions; Atwell et al., 2010) and the French TOU-A local population (192 accessions; Frachon et al., 2017), with a linkage disequilibrium (LD) that decays to $r^2 = 0.5$ within an average of 10 kb and 18 bp, respectively (Frachon et al., 2017; Kim et al., 2007). Importantly, these very small values of LD extent allowed the fine mapping and cloning of genomic regions associated with the natural variation of QDR down to the gene level (Aoun et al., 2020; Huard-Chauveau et al., 2013; Karasov et al., 2014). These two mapping populations were challenged by root inoculation with the *R. solanacearum hpaP* mutant and the corresponding GMI1000 wild-type strain under controlled conditions at 27°C. For the worldwide collection inoculated with GMI1000, we reanalysed the raw data obtained in Aoun et al. (2017) with different statistical models (see section 4). In the worldwide collection, we detected highly significant genetic variation in response to the GMI1000 strain (Figure 1a), with broad-sense heritability estimates being significant 3 days after inoculation (dai) and reaching approximately 0.80 at 7 dai (Table 1). In contrast, when worldwide accessions were inoculated with the *hpaP* mutant, a strong delay in the onset of disease symptoms was observed, with only 12 accessions showing wilting symptoms (Figure 1b). Still, we detected substantial genetic variation in response to the *hpaP* mutant, with significant broad-sense heritability estimates at 8 and 9 dai (8 dai: $H^2 = 0.47$, $p < 0.0001$; 9 dai: $H^2 = 0.64$, $p < 0.0001$; Table 2). The patterns observed in the local mapping population largely differ from the ones observed in the worldwide collection. For instance, in response to GMI1000 or the *hpaP* mutant, local accessions were on average more susceptible than the worldwide accessions (Figure 1). In addition, less genetic variation in response to GMI1000 was detected in the TOU-A population (Figure 1a,c; Tables 1 and 3). When inoculated with the *hpaP* mutant, a delay in the appearance of disease symptoms was still observed in the TOU-A population (Figure 1d). However, in comparison with the worldwide collection, significant natural genetic variation was detected earlier in the TOU-A population, with a broad-sense heritability estimate of 0.44 at 7 dai (Table 4).

2.2 | Genetic basis of response to the *hpaP* mutant largely differs compared to the GMI1000 wild-type strain in both mapping populations

For each mapping population we adopted a genome-wide association approach combined with a local score (GW-LS) analysis (Bonhomme et al., 2019) to finely map the genomic regions

associated with natural variation of response to the GMI1000 wild-type strain and *hpaP* mutant. Following Aoun et al. (2020), we focused in this study on the most significant QTLs (i.e., QTLs containing single-nucleotide polymorphisms [SNPs] with a $-\log_{10}$ (p value) above 5 or a Lindley process value above 20, see section 4). Based on these criteria, we identified in the worldwide collection in response to GMI1000 27 QTLs containing 64 candidate genes (Figure S1, Tables S1 and S2). The most significant SNP (i.e., the top SNP), located in QTL-1, fell into the genomic region of *At3g06090*, a gene encoding a PAMP-induced peptide-like protein (dai = 3, SNP-3-1839089, $p = 2.40 \times 10^{-11}$, local score = 8.6; Table S1). In agreement with previous results described in Aoun et al. (2017), two other top SNPs located in the *RPS4/RRS1* locus (QTL-3, chromosome 5, SNP-5-18325565, SNP-5-18322558, $p = 1.51 \times 10^{-10}$, local score = 31.6) were detected from 6 to 13 dai. Strikingly, this QTL was not detected in response to the *hpaP* mutant, even if the secretion of the PopP2 effector, known to trigger resistance to *R. solanacearum* following its perception by the immune-receptor pair RPS4/RRS1-R (Deslandes et al., 2003), is not altered in this mutant (Lohou et al., 2014). Instead of *RPS4/RRS1*, in the worldwide collection, we detected in response to the *hpaP* mutant 11 QTLs containing 17 candidate genes (Figure 2, Tables S2 and S3), with the top SNP (dai = 9, chromosome 1, SNP-1-17922960, $p = 1.41 \times 10^{-7}$, local score = 4.9) located in QTL-1 containing the genes *At1g48480* and *At1g48490* (Figure 2 and Table S3). *At1g48480* encodes the receptor-like kinase RKL1 (Tarutani et al., 2004), and *At1g48490* encodes the protein kinase IRE3 (for incomplete root hair elongation 3; Yue et al., 2019). Another QTL supported by one top SNP (QTL-4, chromosome 1, SNP-1-17980977, $p = 6.15 \times 10^{-7}$, local score = 5.8) contained four candidate genes, *At1g48625*, *At1g48630*, *At1g48635*, and *At1g48640* (Figure 2 and Table S3). *At1g48625* is a pseudogene, *At1g48640* encodes a transmembrane amino acid transporter family protein, and *At1g48635* encodes PEX3, a peroxine. Interestingly, *At1g48630* encodes RACK1B (receptor for activated c kinase 1B) protein, which acts as a versatile protein involved in multiple biological processes, including functions in disease resistance (Jia et al., 2020).

The number of QTLs was higher in the TOU-A population than in the worldwide collection (Tables S2, S4, and S5). In response to GMI1000, we detected 39 QTLs (containing 192 genes) from 3 to 12 dai (Tables S2 and S4), with the highest association peak located on chromosome 4 (Lindley process = 121.7) and containing three genes (*At4g20070*, *At4g20080*, and *At4g20090*). In response to the *hpaP* mutant, we detected 38 significant QTLs (containing 233 candidate genes) from 7 to 12 dai (Tables S2 and S5). The highest association peak was supported by two top SNPs (QTL-1, chromosome 4, SNP-4-399009 and SNP-4-403181, $p = 4.17 \times 10^{-7}$, local score = 107.3; Table S5). It underlies a large genomic region containing 10 candidate genes (*At4g00893*, *At4g00895*, *At4g00900*, *At4g00905*, *At4g00910*, *At4g00920*, *At4g00930*, *At4g00940*, *At4g00950*, and *At4g00955*). Noteworthy, 22 out of these 38 QTLs were identified at several successive dai, with up to 71 genes
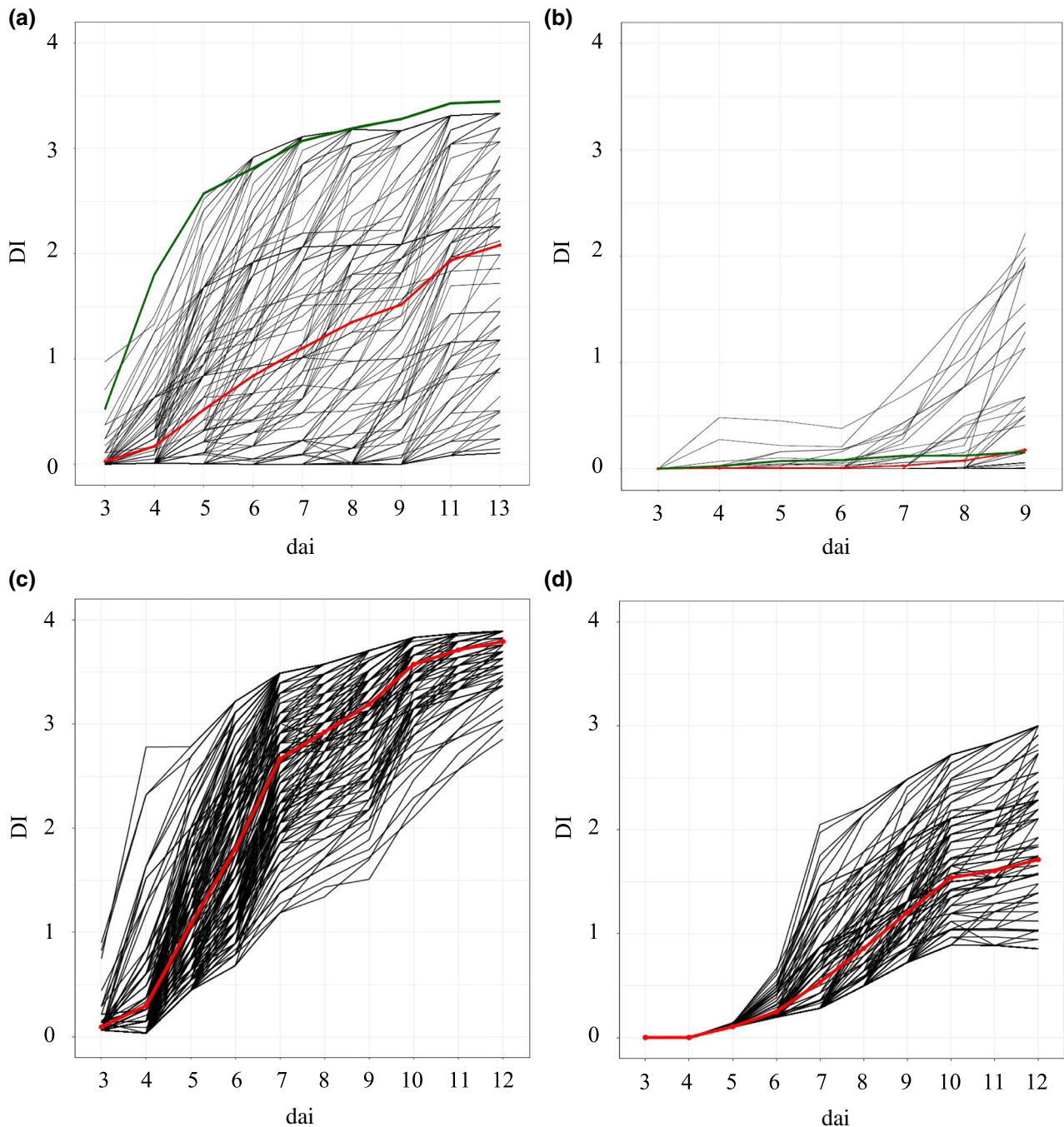
FIGURE 1 Genetic diversity of plant response of two *Arabidopsis thaliana* populations to *Ralstonia solanacearum* inoculation. Worldwide population inoculated with GMI1000 wild-type strain (a) and with the *hpaP* mutant (b). PopTOU-A local population inoculated with GMI1000 wild-type strain (c) and with the *hpaP* mutant (d). For each time point, the best linear unbiased predictors (BLUPS) were estimated using the disease index score values. The red lines represent the mean of the disease index over all the accessions. The green lines represent the mean of the disease index for the Col-0 accession (a, b). Inoculations were performed on 4-week-old plants using the root inoculation method. dai, days after inoculation; DI, disease index

underlying a single QTL, demonstrating the complex genetic basis of the response to the *hpaP* mutant found in the TOU-A population when compared with the worldwide collection.

Importantly, for each mapping population, no detected top SNP was shared between the two strains inoculated, suggesting that the genetic bases of response to GMI1000 and the *hpaP* mutant largely differ whatever the mapping population used.

2.3 | Biological processes identified in the worldwide collection using the *hpaP* mutant seem to involve similar pathways detected in early responses to GMI1000

For each mapping population, the biological processes that were the most significantly represented in candidate gene lists associated

TABLE 1 Natural variation among 161 *Arabidopsis thaliana* accessions of a worldwide collection for disease index in response to *Ralstonia solanacearum* GMI1000 root inoculation

Traits	Symptoms D3		Symptoms D4		Symptoms D5		Symptoms D6		Symptoms D7		Symptoms D8		Symptoms D9		Symptoms D11		Symptoms D13	
Model terms	F or LRT	p	F or LRT	p	F or LRT	p	F or LRT	p	F or LRT	p	F or LRT	p	F or LRT	p	F or LRT	p	F or LRT	p
Accession	25.63	<0.0001	62.94	<0.0001	87.62	<0.0001	132.85	<0.0001	157.51	<0.0001	193.53	<0.0001	172.89	<0.0001	162.37	<0.0001	159.47	<0.0001
Block	3.09	0.0465	3.64	0.0270	5.86	0.0031	7.89	0.0004	5.14	0.0062	8.24	0.0003	7.83	0.0005	5.57	0.0040	5.57	0.0040
Broad-sense heritability H^2	**0.39**		**0.45**		**0.61**		**0.72**		**0.77**		**0.80**		**0.79**		**0.79**		**0.79**	

F, F value resulting from the test of fixed effect; LRT, LRT value resulting from the likelihood ratio test; H^2, broad-sense heritability values; D, days after inoculation; ns, not significant. Numbers in bold indicate significance.

TABLE 2 Natural variation among 164 *Arabidopsis thaliana* accessions of a worldwide collection for disease index in response to *Ralstonia solanacearum hpaP* root inoculation

Traits	Symptoms D3		Symptoms D4		Symptoms D5		Symptoms D6		Symptoms D7		Symptoms D8		Symptoms D9	
Model terms	F or LRT	p	F or LRT	p	F or LRT	p	F or LRT	p	F or LRT	p	F or LRT	p	F or LRT	p
Accession	ns		13.51	0.0002	14.68	0.0001	15.16	<0.0001	5.85	0.0156	21.02	<0.0001	60.99	<0.0001
Block	ns		3.81	0.0101	4.11	0.0067	3.51	0.0151	2.69	0.0455	3.20	0.0231	1.23	0.2994
Broad-sense heritability H^2	ns		0.26		0.18		0.15		0.28		**0.47**		**0.64**	

F, F value resulting from the test of fixed effect; LRT, LRT value resulting from the likelihood ratio test; H^2, broad-sense heritability values; D, days after inoculation; ns, not significant. Numbers in bold indicate significance.

TABLE 3 Natural variation among 182 *Arabidopsis thaliana* accessions of a local TOU-A population for disease index in response to *Ralstonia solanacearum* GMI1000 root inoculation

Traits	Symptoms D3		Symptoms D4		Symptoms D5		Symptoms D6		Symptoms D7		Symptoms D8		Symptoms D9		Symptoms D10		Symptoms D11		Symptoms D12	
Model terms	F or LRT	p	F or LRT	p	F or LRT	p	F or LRT	p	F or LRT	p	F or LRT	p	F or LRT	p	F or LRT	p	F or LRT	p	F or LRT	p
Accession	7.21	0.0073	77.21	<0.0001	42.96	<0.0001	60.04	<0.0001	41.60	<0.0001	37.58	<0.0001	41.40	<0.0001	28.76	<0.0001	18.31	<0.0001	8.46	0.0003
Block	0.62	0.5377	3.65	0.0265	12.90	<0.0001	15.98	<0.0001	16.26	<0.0001	17.48	<0.0001	13.32	<0.0001	12.30	<0.0001	9.22	0.0001	7.08	0.0009
Broad-sense heritability H^2	**0.46**		**0.68**		**0.55**		**0.59**		**0.52**		**0.50**		**0.53**		**0.47**		**0.43**		**0.37**	

F, F value resulting from the test of fixed effect; LRT, LRT value resulting from the likelihood ratio test; H^2, broad-sense heritability values; D, days after inoculation; ns, not significant. Numbers in bold indicate significance.

TABLE 4 Natural variation among 172 *Arabidopsis thaliana* accessions of a local TOU-A population for disease index in response to *Ralstonia solanacearum* hpaP root inoculation

Traits	Symptoms D3		Symptoms D4		Symptoms D5		Symptoms D6		Symptoms D7		Symptoms D8		Symptoms D9		Symptoms D10		Symptoms D11		Symptoms D12	
Model terms	F or LRT	p	F or LRT	p	F or LRT	p	F or LRT	p	F or LRT	p	F or LRT	p	F or LRT	p	F or LRT	p	F or LRT	p	F or LRT	p
Accession	ns		26.23	<0.0001	13.19	0.0003	8.14	0.0043	11.94	0.0006	11.86	0.0006	15.84	<0.0001	22.51	<0.0001	18.72	<0.0001	29.76	<0.0001
Block	ns		1.01	0.3664	1.75	0.1745	1.64	0.1943	1.85	0.1578	0.94	0.3914	2.39	0.0922	1.73	0.1777	0.96	0.3835	0.92	0.4003
Broad-sense heritability H^2	ns		**0**		**0.02**		**0.19**		**0.44**		**0.44**		**0.46**		**0.50**		**0.48**		**0.54**	

F, F value resulting from the test of fixed effect; LRT, LRT value resulting from the likelihood ratio test; H^2, broad-sense heritability values; D, days after inoculation; ns, not significant. Numbers in bold indicate significance.
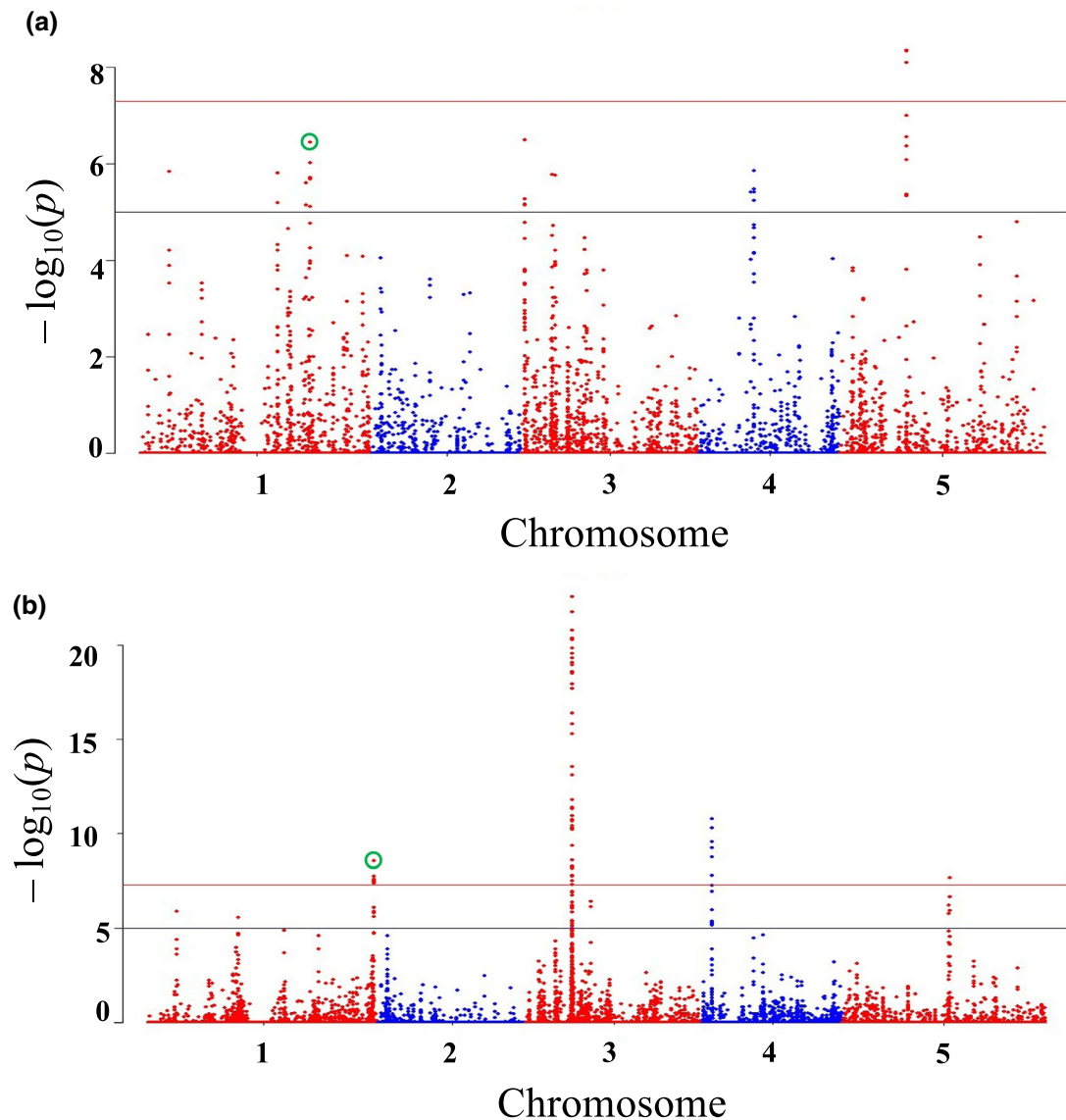
FIGURE 2 The genetics of quantitative disease resistance to *Ralstonia solanacearum hpaP* mutant in the worldwide population identified by GW-LS mapping. Whole-genome scan of 214, 051 single-nucleotide polymorphisms (SNPs) for association with the disease index at 8 days after inoculation (dai) (a) and 9 dai (b). The green circles highlight the top SNPs corresponding to QTL-1 (a) and QTL-4 (b) on chromosome 1, highlighting *At1g48480* and *At1g48490* genes for QTL-1 and *At1g48630* and At1g48635 genes for QTL-4

with the top SNPs detected for GMI1000 and the *hpaP* mutant were analysed with the classification superviewer tool using the MapMan classification as the source (http://www.bar.utoronto.ca/ntools/cgi-bin/ntools_classification_superviewer.cgi) (Figures 3 and S4, Table S2). For the worldwide collection, response to GMI1000 corresponded to genes mostly involved in redox, DNA, protein and lipid metabolisms, stress response, and signalling (Figure 3 and Table S2). In agreement with the delay in the onset of disease symptoms observed in response to the *hpaP* mutant (Figure 1), biological processes including hormone and lipid metabolisms found enriched at 3 dai in response to GMI1000 were also enriched in response to the *hpaP* mutant, but at later time points of the kinetics (8 and 9 dai).

Although the identity of the underlying genes was different, they were classified in the same metabolic pathway on structured annotation criteria (MapMan classification).

For the TOU-A population, DNA, RNA, protein, and polyamine metabolisms were significantly enriched in response to both strains (Figure S4). Still, the identity of the underlying genes was different between the strains (Table S2). In addition, miscellaneous processes as well as glycolysis and transport metabolism, enriched at 11 and 12 dai, appeared to be specific to the response to the *hpaP* mutant.

Overall, the biological processes involved in response to the two strains appear to be more similar in the TOU-A population (Figure S4) than in the worldwide collection (Figure 3).
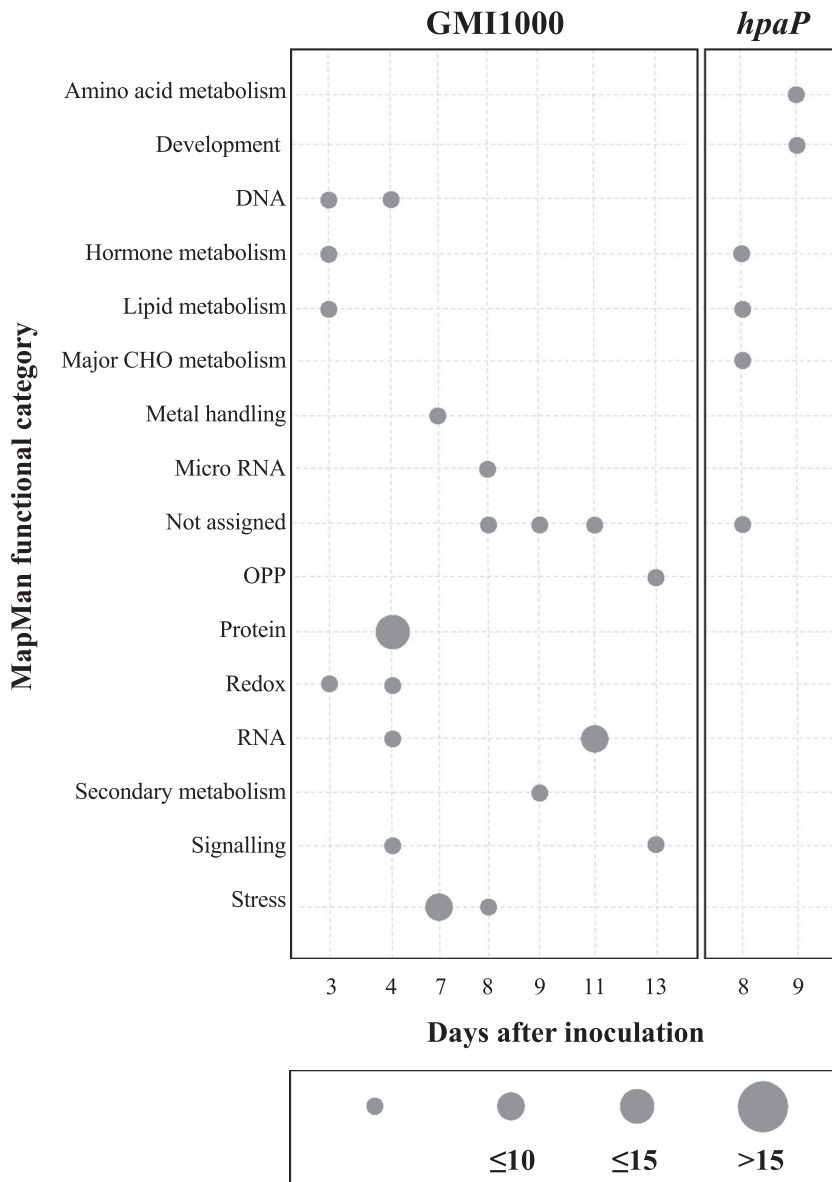
FIGURE 3 Enriched pathways for the candidate gene lists associated with the top single-nucleotide polymorphisms (SNPs) detected in the worldwide collection inoculated with the GMI1000 wild-type strain and *hpaP* mutant, obtained with MapMan Classification Super Viewer. The size of the dots corresponds to the number of candidate genes in each category

2.4 | *RKL1*, *RACK1B*, and *PEX3* are involved in *R. solanacearum* HpaP-dependent plant susceptibility

Due to the greater complexity of the genetic architecture of the response to the *hpaP* mutant observed in the TOU-A population, we decided to validate some candidate genes identified in the worldwide collection. These candidate genes were annotated to have functions that could be related to plant defence response and underlie the most significant QTLs. As a first step, we selected two of the most resistant (Bu-0 and CIBC-5) and susceptible (Lm-2 and Nok-3) worldwide accessions to the *hpaP* mutant. After inoculation with the *hpaP* mutant, we confirmed phenotypic differences, with susceptible accessions exhibiting severe disease development (least-square [LS] means of disease index scores at 9 dai of 3.65 and 3.26 for Lm-2 and Nok-3, respectively) in comparison with resistant accessions that remained symptomless (Figure 4a,c, Tables S6 and S7). In addition, disease development was associated with a

massive bacterial multiplication in the susceptible accessions compared to the resistant ones, with three to four log of differences (Figure 4b).

Then, we evaluated in these four accessions the natural expression profiles of four candidate genes underlying the QTL-1 (*RKL1*, *IRE3*) and QTL-4 (*RACK1B*, *PEX3*) identified in the worldwide collection (Table S8). Using quantitative reverse transcription PCR (RT-qPCR), gene expression was measured at 7 dai, thereby corresponding to 1 day before the detection of QTL-1 and QTL-4. Interestingly, three out of these four candidate genes showed a significantly differential expression level between the resistant and susceptible accessions (Figure 5 and Table S9). *RKL1* and *RACK1B* were more expressed in Bu-0 and CIBC-5 resistant accessions than in Lm-2 and Nok-3 susceptible accessions (Figure 5a,c). Conversely, *IRE3* was more expressed in the susceptible accessions than in the resistant accessions (Figure 5b). *PEX3* expression was similar among the four accessions (Figure 5d).
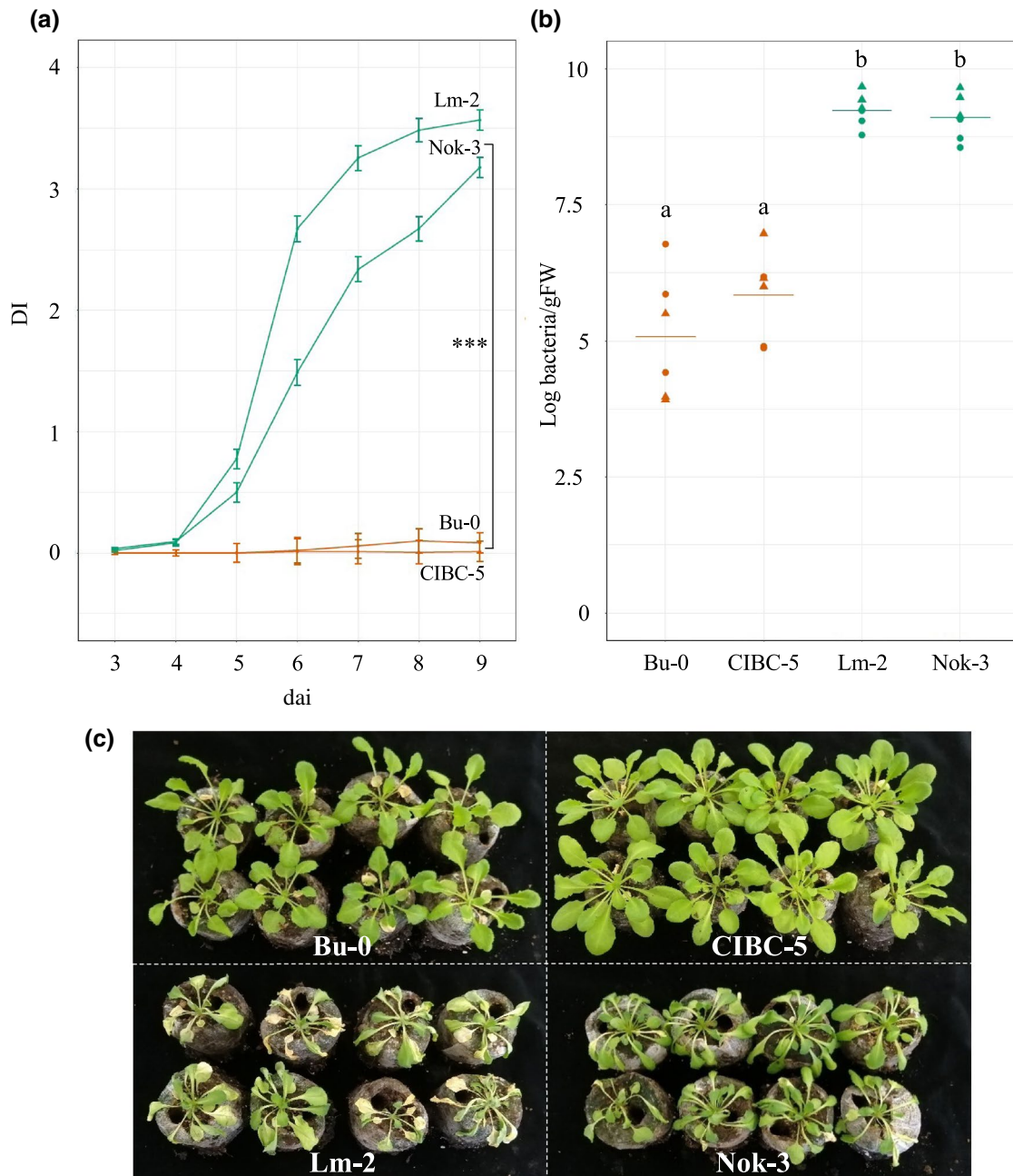
FIGURE 4 Comparison of wilting symptoms and in planta bacterial measurement of two resistant (Bu-0 and CIBC-5) and two susceptible (Lm-2 and Nok-3) *Arabidopsis thaliana* accessions following root inoculation with *Ralstonia solanacearum hpaP* mutant. (a) Dynamics of disease symptoms at 9 days after inoculation (dai). Least-square (LS) means ± standard error of the LS means (Table S6) from two independent inoculations ($n = 72$ plants per genotype, ***$p < 0.001$). Statistical analysis results are presented in Table S7. (b) In planta bacterial multiplication in *A. thaliana* rosettes. Number of colony-forming units (CFU) per gram of fresh weight (FW) of rosettes harvested at 7 dai, a time point corresponding to an average disease index of 3 for the susceptible accessions (Lm-2, Nok-3). Three pools of three plants were used with two independent repetitions. A Tukey's test was performed ($F = 49.35$, $p < 0.0001$) and treatments with the same letter are not significantly different. (c) Representative pictures taken at 8 dai. DI, disease index; green, susceptible accessions; dark orange, resistant accessions

Finally, we selected publicly available T-DNA insertion mutants for these four genes. T-DNA insertions were confirmed by genotyping and sequencing the T-DNA flanking sequences and homozygous progenies were produced (Figure S5). Corresponding mutants were phenotyped following root inoculation with the

hpaP mutant. While no or barely significant difference was observed between these mutant lines and the corresponding wild-type accession Col-0 (Figure S6, Tables S10 and S11), the four genes appear not to be involved in the resistance to *hpaP* mutant. Meanwhile, we could not exclude a role of these genes
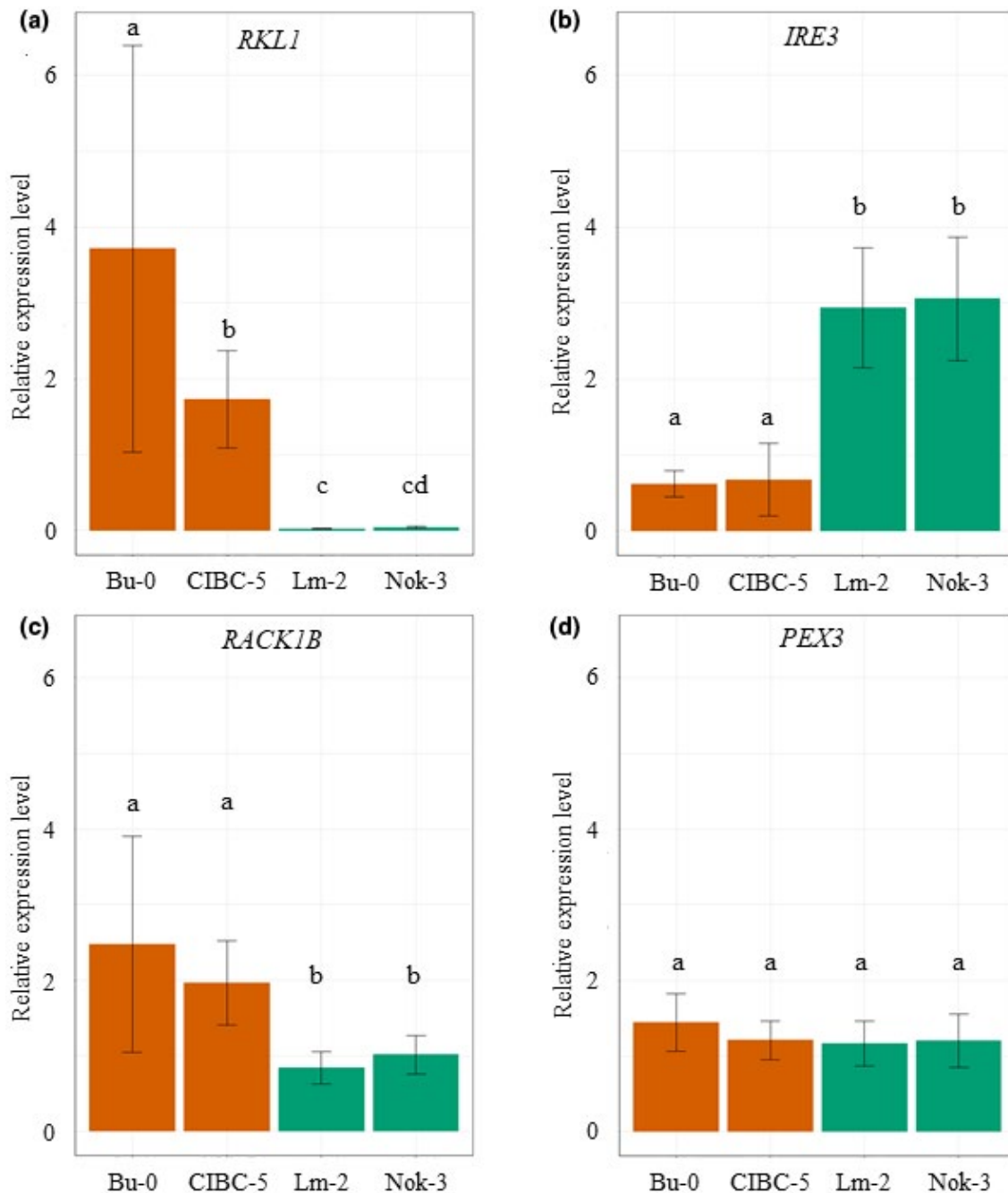
FIGURE 5 Relative expression level of four candidate genes from GW-LS mapping with the *Arabidopsis thaliana* worldwide population inoculated with *Ralstonia solanacearum hpaP* mutant in two resistant (Bu-0 and CIBC-5) and two susceptible (Lm-2 and Nok-3) accessions at 7 days after inoculation (dai). (a) *At1g48480*, (b) *At1g48490*, (c) *At1g48630*, and (d) *At1g48635*. Statistical analyses were performed using Tukey's test and treatments with the same letter are not significantly different (Table S9). Green, susceptible accessions; dark orange, resistant accessions

in susceptibility to *R. solanacearum*. To test this hypothesis, we phenotyped the same mutant lines with the GMI1000 strain, using the susceptible corresponding Col-0 accession as a control (Figure 6a–e, Tables S12 and S13). No or a slight significant difference was observed in disease establishment for the two *ire3* mutant lines (Figure 6a,b), corroborated by the absence of difference in in planta bacterial multiplication when compared to Col-0 (Figure 6f). By contrast, for the three other mutant lines, *pex3*

(Figure 6c), *rack1b* (Figure 6d), and *rkl1* (Figure 6e), a strong delay in the disease appearance was observed compared to Col-0, with fewer symptoms observed after 11 dai. This loss of susceptibility was associated with a significant impairment of bacterial multiplication in the *rack1b* and *rkl1* mutants (Figure 6f). Altogether, these data indicate that RKL1, RACK1B, and PEX3 are *R. solanacearum* targets contributing to quantitative disease establishment, probably in an HpaP-dependent manner.
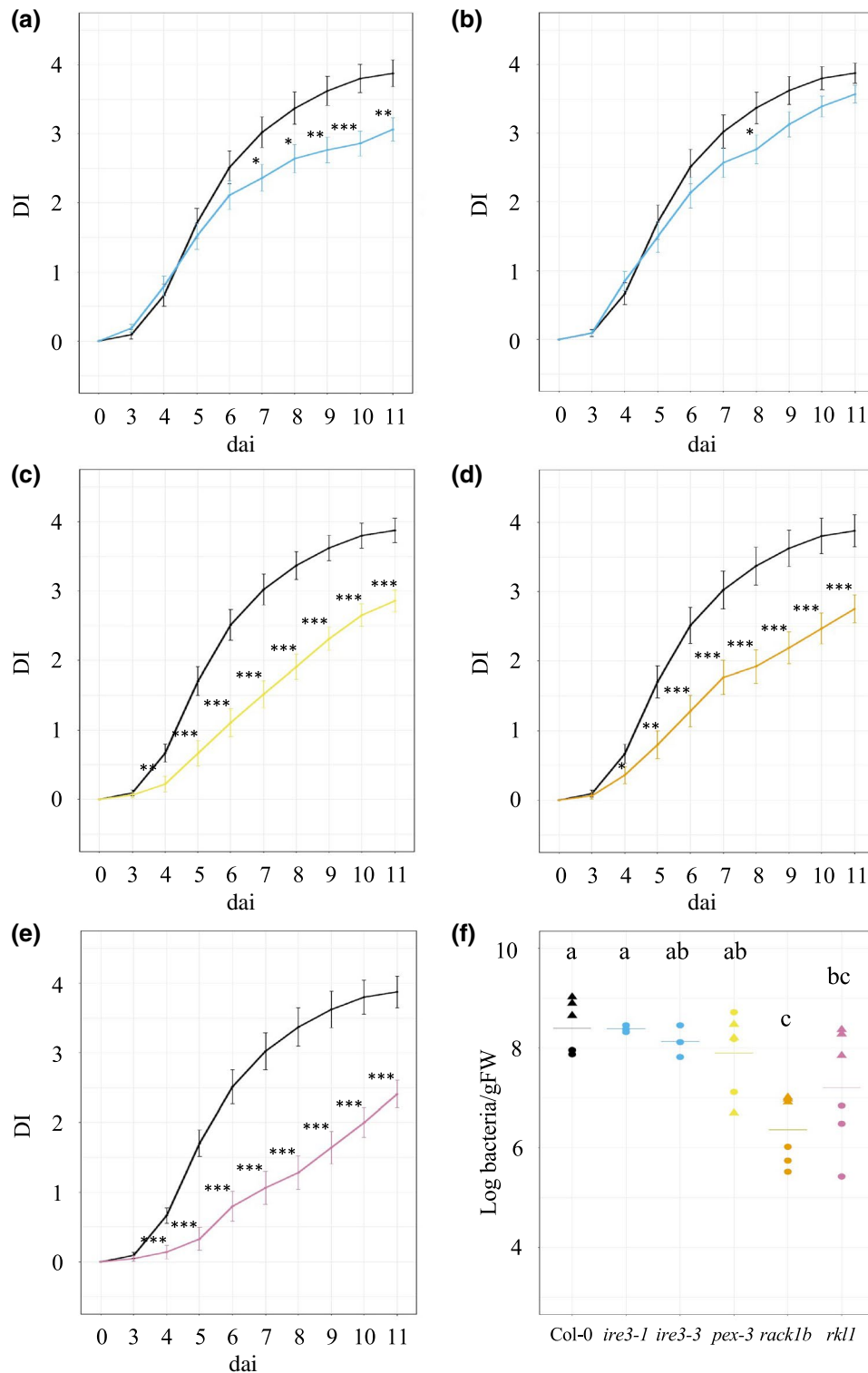
FIGURE 6 Dynamics of disease symptoms and in planta bacterial multiplication after *Ralstonia solanacearum* GMI1000 wild-type inoculation of selected *Arabidopsis thaliana* mutant lines. (a–e) Disease index curves 11 days after inoculation (dai) of the mutant lines compared to the Col-0 control (in black). Responses of two *ire3* mutants (a, b), *pex3* mutant (c), *rack1b* mutant (d), and *rkl1* mutant (e). Least-square means ± standard errors from two independent replicates (*n* = 32 plants per genotype) and analysis of variance associated are presented in Tables S12 and S13 (*$p < 0.05$, **$p < 0.01$, ***$p < 0.001$). DI, disease index. (f) In planta bacterial multiplication in *A. thaliana* rosettes of the wild-type Col-0 and different mutant lines. Number of colony-forming units (CFU) per gram of fresh weight (FW) of rosettes harvested at 6 dai, a time point corresponding to an average disease index of 3 for Col-0. Three pools of three plants were used with two independent repetitions or with two alleles for *ire3* mutant. A Tukey's test was performed (*F* = 5.91; *$p < 0.001$*) and treatments with the same letter are not significantly different

3 | DISCUSSION

To date, most GWAS on the natural genetic variation of plant response to pathogens were based on wild-type pathogenic strains, which were mainly isolated from crops (Badet et al., 2019; Bartoli & Roux, 2017; Rajarammohan et al., 2018). Alternatively, studying the impact of a single bacterial protein on plant response was recently used in GWAS. For instance, *Pseudomonas syringae* HopAM1 T3E or the HrpJ type III syringe component were specifically delivered by a disarmed *Pseudomonas fluorescens* strain (Iakovidis et al., 2016; Lonjon et al., 2020). While this reductionist approach is quite powerful, it might be not ecologically realistic. In this study, we proposed another approach by challenging two complementary mapping populations to a *R. solanacearum* mutant in which a major pathogenic determinant was defective. Therefore, this approach focuses on the potential effect of a single pathogenicity determinant while keeping the entire bacterial genomic background intact.

A growing number of studies elucidated the function of some pathogenicity determinants of *R. solanacearum*, among which most are T3Es (Landry et al., 2020). A *R. solanacearum* mutant lacking HpaP resulted in a unique plant phenotype when inoculated on the widely used *A. thaliana* Col-0 susceptible genotype (Lohou et al., 2014), a rare phenotype when compared to single T3E mutant studies (Cunnac et al., 2004; Peeters et al., 2013). In this study, by adopting this new approach, we refined the role of the *R. solanacearum* HpaP T3S4 protein by highlighting plant genes specifically modulated by HpaP.

3.1 | A delayed response of two *A. thaliana* mapping populations to the *hpaP* mutant

In both *A. thaliana* mapping populations, we observed a delay in disease establishment with the *hpaP* mutant in comparison with the GMI1000 wild-type strain. Accordingly, some biological processes found enriched at the late stage of the kinetics with the *hpaP* mutant were similar to the ones found at the early stage of the infection with GMI1000, notably for the worldwide collection. In this case, they correspond to hormone and lipid metabolisms, though the genes underlying these processes remained different.

In a previous study we observed similar secretome patterns between GMI1000 and *hpaP* mutant, with the exception of four and two early type III-associated substrates, which were significantly less or more secreted by the *hpaP* mutant, respectively (Lonjon et al., 2020). These slight differences in the secretome or probably other effects related to the absence of the HpaP T3S4 protein, such as putative posttranslational modification of other secreted proteins, could explain this global delay in response to the mutant. However, the posttranscriptional and posttranslational mechanisms taking place in the fine control and hierarchy of the secretion are far from being understood (Büttner, 2012).

3.2 | The playful dynamic genetic architecture of QDR depends on *hpaP* and the mapping population

Reminiscent of phenological traits scored on both the worldwide collection and the TOU-A local population (Brachi et al., 2013), the extent of genetic variation and the underlying genetic architecture were highly dependent on the type of mapping population. In comparison with the local mapping population, the genetic diversity of response to both strains was more contrasted in the worldwide collection; the majority of the accessions remained symptomless with the *hpaP* mutant while all the accessions were more susceptible in the local population. Whether this increased susceptibility is specific to the TOU-A local population remains an open question that would deserve the phenotyping of an extensive number of other French natural populations in response to both GMI1000 and the *hpaP* mutant, such as the set of 168 natural populations located in south-west France (Frachon et al., 2018, 2019). Knowing that Hpa proteins are important for the *R. solanacearum* infection process in T3S establishment and T3E secretion (Lonjon et al., 2016, 2020), we propose that the strong phenotypic differences observed especially in the worldwide collection to the mutant could highlight the early HpaP modulated plant response. In addition, for both strains, the genetic architecture was more complex in the local population than in the worldwide collection and no top SNPs were common between these two mapping populations. Several nonexclusive hypotheses can be proposed to explain this discrepancy. First, in agreement with a shorter linkage disequilibrium observed in the local population (i.e. 18 bp; Frachon et al., 2017) than in the worldwide collection (about 10 kb; Atwell et al., 2010), the effect of population structure is much more pronounced in the worldwide collection (Brachi et al., 2013). While appropriate statistical methods used to correct for strong confounding by population structure reduce the rate of false-positive associations, they also increased the rate of false negatives (i.e., causative SNPs that are lost as an artefact of population structure corrections), thereby decreasing the power to detect QTLs in the worldwide collection (Bergelson & Roux, 2010; Brachi et al., 2010). Second, in agreement with the strong population genetic differentiation observed in *A. thaliana* (Platt et al., 2010), both genetic heterogeneity and/or allelic heterogeneity are expected to be more important in the worldwide collection than in the TOU-A population, with the fixation of different mutations related to the same phenotypic trait among different populations. These heterogeneities in turn limit the power of detection of QTLs (Bergelson & Roux, 2010). Third, the level of phenotypic and genetic variation of QDR to the *R. solanacearum* GMI1000 wild-type strain was suggested to be related to the absence of fully resistant accessions in the TOU-A local population compared to the worldwide collection, in which a major association peak corresponding to the *RPS4/RRS1-R* locus was detected (Aoun et al., 2017, 2020). This locus encodes an immune-receptor pair mediating one of the main sources of resistance to different strains of *R. solanacearum* (Deslandes et al., 1998). A similar assumption could be made for the difference observed in natural variation of QDR to the *hpaP* mutant because we previously

showed that PopP2, the T3E perceived by RSP4/RRS1-R (Deslandes et al., 2003; Le Roux et al., 2015), was still fully secreted and translocated by the *hpaP* mutant (Lohou et al., 2014; Lonjon et al., 2020). However, we did not detect this locus in the worldwide collection inoculated with *hpaP*. Interestingly, although none of the candidate genes underlying QTLs were common between the two strains, we observed that a majority of the enriched biological processes were common and found enriched at the same time point, in particular in the local population. These findings demonstrate (a) that the study of the natural diversity of plant response to a pathogen single mutant is an original and powerful strategy to identify new plant genes targeted by a pathogen, and (b) that HpaP, as a key regulator of early substrates of the T3SS, is a robust choice to reveal important QTLs involved in *R. solanacearum* response, QTLs potentially hidden in a wild-type context by the major *RRS1-R/RPS4* locus.

To gain more knowledge on the function of the genes underlying QTLs identified, we explored their expression profiles using publicly available expression studies on the Genevestigator tool. Consistently, whatever the candidate genes considered and the strains used, they are strongly up-regulated in biotic stress experiments involving bacterial and fungal pathogens such as *P. syringae* pv. *maculicola* (Bernsdorff et al., 2016), *Blumeria graminis* (Maekawa et al., 2012), and *Botrytis cinerea* (Liu et al., 2015). As mentioned above, while hormone and lipid metabolism pathways are enriched in response to both strains for the worldwide collection, none of the genes falling into these groups are common, although some of them have been related to the plant response to pathogens. For instance, for hormone metabolism, *At3g23240* identified in response to *hpaP* mutant, encoding ETHYLENE RESPONSE FACTOR1 (ERF1), was previously found to be expressed, along with *PDF1.2* and *CHI/PR3* from jasmonic acid (JA) and ethylene pathways, in response to *Fusarium poae* inoculation (Dinolfo et al., 2017). Alternatively, the bHLH transcription factor MYC2/JIN1 (*At1g05710*), highlighted in response to GMI1000, was described to be a master regulator of diverse JA-mediated responses by antagonistically regulating two distinct branches of the JA signalling pathway in response to necrotrophs (Kazan & Manners, 2013). By contrast, for lipid metabolism, the role of the identified genes remains largely unknown. However, the functional characterization of *AtNCER1*, one of the three *A. thaliana* neutral ceramidases to which *AtNCER3* (*At5g58980*) belongs, suggests these proteins are involved in the homeostasis of sphingolipids, signalling molecules known to participate in the mediation of plant responses to biotic and abiotic stresses (Li et al., 2015). Together, these data underline the relevance of the candidate genes identified, with a diversity of functions mainly related to biotic stress responses.

3.3 | *RKL1, RACK1B,* and *PEX3*: three HpaP-dependent susceptibility genes involved in plant response to *R. solanacearum*

In the worldwide collection challenged with the *hpaP* mutant, we detected 11 QTLs containing 17 genes harbouring a diversity of

putative functions. Among these, we selected two pairs of candidate genes underlying two QTLs, *RKL1* (*At1g48480*)/*IRE3* (*At1g48490*) and *RACK1B* (*At1g48630*)/*PEX3* (*At1g48635*), and functionally validated *RKL1, RACK1B,* and *PEX3* as susceptibility genes in response to *R. solanacearum*. Although *IRE3* expression was significantly higher in the *hpaP* susceptible than in the *hpaP* resistant accessions, the involvement of *IRE3* in the response to *R. solanacearum* remains uncertain because the bacterial multiplication in the two mutant lines, *ire3-1* and *ire3-3*, does not differ from Col-0 despite a significant difference observed in wilting disease kinetics.

RKL1 belongs to the LRR class of receptor-like kinases (RLKs) and *RKL1* is expressed in the vascular tissue of the entire root system, with the *rkl1* mutant showing a reduction in root length (ten Hove et al., 2011). Besides being key regulators of plant architecture and growth, RLKs also play a role in defence and stress responses (Marshall et al., 2012). For instance, previous studies identified the RLK *ERECTA* gene as being involved both in plant development (Torii et al., 1996) and in QDR to bacterial wilt (Godiard et al., 2003). Interestingly, both RKL1 and RLK902 (*At3g17840* gene, closest *RKL1* homolog) were found to interact with EDR4 (ENHANCED DISEASE RESISTANCE 4), an *A. thaliana* protein involved in plant immunity, either having a negative or positive role in resistance to powdery mildew pathogen *Golovinomyces cichoracearum* or to *P. syringae*, respectively (Wu et al., 2015; Zhao et al., 2019). Moreover, *RLK902* is involved in resistance to the bacterial pathogen *P. syringae* (Zhao et al., 2019). By contrast, *rkl1* mutant harboured a significant delay in disease establishment and in planta bacterial multiplication was significantly reduced. We cannot exclude that this difference in phenotype may also be due to a defect in root development that could affect the bacterial infection. This is another example of the diversity of functions of RLKs in plant response, potentially acting in resistance or susceptibility according to the pathogen encountered.

Of the two other functionally validated candidate genes, *RACK1B* was found to be involved in plant immune responses. *RACK1B* shares about 90% identity with *RACK1A* and *RACK1C*, these three *A. thaliana* homologous genes (Chen, 2006) encoding RACK1 (Receptor for Activated C Kinase 1) proteins, which are members of the tryptophan-aspartate repeat (WD-repeat) family, playing a role in shuttling, anchoring proteins at specific locations, and stabilizing protein activity (Adams et al., 2011). RACK1 is involved in the bacterial damage-associated molecular pattern (DAMP)-triggered immune pathway, being an essential component of a new immune signalling pathway in *A. thaliana* activated by pathogen-secreted proteases (Cheng et al., 2015). In addition, by its participation in the scaffolding of multiprotein complexes, leading to numerous interactions with various ligands among which are many immune proteins, RACK1 emerged as an important actor of defence against pathogens in plants (Islas-Flores et al., 2015). Hormones are known to play a decisive role in the establishment of bacterial wilt. For example, several *A. thaliana* mutants of genes involved in abscisic acid (ABA) signalling (*abi1-1, abi2-1,* and *aba1-6*) were described as becoming more susceptible to *R. solanacearum* (Hernández-Blanco et al., 2007). Alternatively, the *ein2-1* (ethylene insensitive 2) mutant impaired in

ethylene signalling showed a delay in bacterial wilt establishment with several virulent strains of *R. solanacearum* in *A. thaliana* (Hirsch et al., 2002). Interestingly, RACK1 is also implicated in the regulation of plant response to ABA (Guo et al., 2009), and RACK1 and EIN2 were found to genetically interact to regulate plant growth and development in *A. thaliana* (Wang et al., 2019). In the same line, the *PEX3* gene, which participates in peroxisome biogenesis and plant antioxidant networks, has been recently identified as an important factor in the drought tolerance response involving ABA (Ebeed et al., 2018). Another peroxisome biogenesis gene, *PEX1*, is induced in response to wounding and infection with *P. syringae* (Lopez-Huertas et al., 2000). In addition, the results obtained for PEX3 also support the finding that its manipulation by the bacterium does not rely on its transcriptional regulation.

Susceptibility genes are classically defined as any plant gene that facilitates the infection process or supports compatibility with a pathogen (van Schie & Takken, 2014; Zaidi et al., 2018). Altogether, our data validated RACK1B, PEX3, and RKL1 as susceptibility factors manipulated by *R. solanacearum* in the early steps of the infection in an HpaP-dependent manner. In the same way, most of the genes validated in previous GWAS studies with *R. solanacearum* correspond to susceptibility genes (Aoun et al., 2017, 2020). Such genes, manipulated by pathogens to facilitate their multiplication, have been suggested as robust sources of resistance if disrupted in plants (van Schie & Takken, 2014; Zaidi et al., 2018). Alternatively, QDRs were suggested to confer durable and broad-spectrum resistance against numerous pathogen species (Debieu et al., 2016; French et al., 2016; Roux et al., 2014). However, the literature shows that their spectrum of action has to be carefully considered, as some plant genes have been described as being involved either in resistance or susceptibility according to the interacting pathogen (Lorang et al., 2012; Zhao et al., 2019). One direct perspective of this work will be to further characterize susceptibility genes and to evaluate their spectra of action.

4 | EXPERIMENTAL PROCEDURES

4.1 | Bacterial strains, plant material, and growth conditions

The *R. solanacearum* GMI1000 wild-type strain and *hpaP* mutant were grown as described by Lohou et al. (2014). When needed, kanamycin (50 mg/L) was added. To investigate the natural variation of response of *A. thaliana* to *R. solanacearum*, two sets of *A. thaliana* wild accessions were used. The first set corresponds to 176 accessions from a worldwide collection (Atwell et al., 2010), while the second set corresponds to 192 whole-genome sequenced accessions of the French TOU-A population (Frachon et al., 2017). Detailed information on the *A. thaliana* T-DNA insertion mutants used in this study, corresponding to the *At1g48480*, *At1g48490*, *At1g48630*, and *At1g48635* genes, is listed in Table S8. They were identified using the T-DNA express *Arabidopsis* online mapping tool (http://signal.salk.

edu/cgi-bin/tdnaexpress; Alonso et al., 2003) and ordered from the Nottingham Arabidopsis Stock Centre (University of Nottingham, UK). All the mutants analysed in this study are in the Columbia accession background (Col-0, NASC ID CS70000). *A. thaliana* accessions and mutants were grown as described in Aoun et al. (2017).

4.2 | Plant inoculation and phenotyping

Inoculations on intact roots were performed as previously described (Lohou et al., 2014). Briefly, plants were soaked for 20 min in 2 L per tray of a bacterial suspension at 10^8 cfu/ml. Inoculated plants were then transferred to a growth chamber at 27°C (75% relative humidity [RH], 12 h light, at 100 μmol·m^{-2}·s^{-1}). Plants were monitored for wilting symptoms from 3 to 11 days after inoculation (dai) with a disease index scale ranging from 0 (healthy plants) to 4 (dead plants) (Morel et al., 2018).

4.3 | Natural variation of response of the two *A. thaliana* mapping populations to *R. solanacearum*

4.3.1 | Experimental design

For the worldwide collection inoculated with the GMI1000 wild-type strain, raw phenotyping data produced in Aoun et al. (2017) at 27°C on intact roots were retrieved for 161 accessions. For the *hpaP* mutant, we adopted a randomized complete block design (RCBD) of two experiments each consisting of two blocks containing one replicate of 164 and 113 accessions, respectively.

For the TOU-A population, 182 and 172 accessions were phenotyped in response to the GMI1000 wild-type strain and *hpaP* mutant, respectively. For each strain, the plants were arranged according to a RCBD of three experimental blocks, each containing one replicate of each accession.

4.3.2 | Statistical analysis

For each mapping population × *R. solanacearum* strain combination, a mixed model was used to explore the natural genetic variation of the disease index at each time point of phenotyping using the "lme4" library under the R environment (R Studio Team, 2020), as follows:

$$\text{disease index}_{ijc} = \mu + \text{block}_i + \text{accession}_j + \varepsilon_{ijc} \qquad (1)$$

where μ is the overall mean of the phenotypic data, "block" accounts for differences in micro-environmental conditions between the experimental blocks used, "accession" corresponds to the genetic differences among the worldwide or the TOU-A natural accessions, and ε is the residual term. The factor "block" was considered as a fixed factor and the factor "accession" as a random factor. The significance of the random effect was determined by likelihood ratio tests of the model with and

without this effect. Residuals were normally distributed so no transformation was applied on raw phenotypic data. For each natural accession, we estimated best linear unbiased predictors (BLUPs) obtained for each natural accession. Because *A. thaliana* is a highly selfing species (Platt et al., 2010), BLUPs correspond to genotypic values. Using a formula adapted from Gallais (1990), broad-sense heritability (H^2) at each time point of phenotyping was estimated from variance component estimates for the "block" and "accession" terms obtained with the "lme4" and "lmtest" libraries under the R environment (R Studio Team, 2020).

4.3.3 | GWA mapping with local score analysis

For each mapping population × *R. solanacearum* strain combination, genomic regions associated with natural disease index variation at each time of phenotyping were mapped by using a mixed model implemented in the software EMMAX (Efficient Mixed-Model Association eXpedited; Kang et al., 2010). To control for the effect of population structure, we included as a covariate an identity-by-state kinship matrix K. This kinship matrix is based on 214,051 SNPs evenly spaced across the genome for the worldwide collection (Horton et al., 2012) and on 1,902,592 identified SNPs for the TOU-A mapping population (Frachon et al., 2017). Rare alleles may increase the rate of false positives (Atwell et al., 2010). Therefore, based on previous GWAS performed on the two mapping populations, we only considered SNPs with a minor allele relative frequency (MARF) >10% in the worldwide collection (Brachi et al., 2010; Kang et al., 2010) and >7% in the TOU-A population (Frachon et al., 2017).

To better characterize the genetic architecture associated with the natural genetic variation of disease index, we followed the procedure described in Aoun et al. (2020) by applying a local score approach on the set of *p* values provided by EMMAX. This local score approach increases the power of detecting QTLs with small effect and narrows the size of QTL genomic regions (Bonhomme et al., 2019). In this study, we used a tuning parameter ξ of 2. Based on the procedure described in Aoun et al. (2020), we focused on QTLs containing SNPs with a $-\log_{10}(p$ value) above 5 or a Lindley process value above 20 with a heritability above 0.30. We considered as candidate all the genes falling in a ± 2 kb window of each top SNP.

4.4 | In planta bacterial multiplication

For each experiment, the rosettes of three pools of three *A. thaliana* plants were harvested for each accession or mutant line, at a time point corresponding to an average disease index of 3 for the susceptible accessions Lm-2, Nok-3, or Col-0. Leaves were sterilized for 1 min in 70% ethanol solution and washed three times for 1 min in sterile water. Pools of three plants were then weighed and ground using a pestle and mortar, and resuspended in 5 ml of sterile water. Bacterial concentrations were determined by plating serial dilutions on B medium with antibiotics when necessary. Experiments were repeated twice.

4.5 | Validation of T-DNA insertion mutations

For each T-DNA insertion mutant line (Table S8), six to 12 plants were genotyped to confirm the T-DNA insertion and to select homozygous mutants. Leaf samples were harvested and DNA extracted as described in Mayjonade et al. (2016). Primers used for genotyping, listed in Table S14, were identified with the SALK T-DNA primer online tool (http://signal.salk.edu/tdnaprimers.2.html). The PCR mix was composed as described in Aoun et al. (2017). The PCR cycling conditions were as follow: 95°C for 2 min; a high-temperature phase of 10 cycles at 95°C for 30s, 62–52°C for 30 s (touchdown, 1°C decrease at each cycle), and 72°C for 1 min; a lower temperature phase of 30 cycles at 95°C for 30 s, 52°C for 30 s, and 72°C for 1 min; then 72°C for 2 min.

4.6 | RNA extraction and RT-qPCR

RNA extractions and RT-qPCR analyses were performed as described (Le Roux et al., 2015). Each experiment was composed of two biological replicates each containing three technical qPCR replicates. A first experiment was realized to analyse the expression profile of *At1g48480*, *At1g48490*, *At1g48630*, and *At1g48635*. For each repetition, a pool of three leaves from three plants for each accession was harvested at 7 dai from plants inoculated with water or the *hpaP* mutant. A second experiment was performed to check the expression level of the gene interrupted by the T-DNA insertion for the mutant selected. In this case, a pool of four leaves corresponding to four plants was harvested. Corresponding primers are listed in Table S14.

DATA AVAILABILITY STATEMENT
The data that support the findings of this study are available from the corresponding author upon reasonable request.

ORCID
Fabrice Roux https://orcid.org/0000-0001-8059-5638
Fabienne Vailleau https://orcid.org/0000-0002-6879-2695

REFERENCES
Adams, D.R., Ron, D. & Kiely, P.A. (2011) RACK1, A multifaceted scaffolding protein: structure and function. *Cell Communication and Signaling*, 9, 22.

Alonso, J.M., Stepanova, A.N., Leisse, T.J., Kim, C.J., Chen, H., Shinn, P. et al. (2003) Genome-wide insertional mutagenesis of *Arabidopsis thaliana*. *Science*, 301, 653–657.

Alonso-Díaz, A., Satbhai, S.B., de Pedro-Jové, R., Berry, H.M., Göschl, C., Argueso, C.T. et al. (2021) A genome-wide association study reveals cytokinin as a major component in the root defense responses against *Ralstonia solanacearum*. *Journal of Experimental Botany*, 72, 2727–2740.

Aoun, N., Desaint, H., Boyrie, L., Bonhomme, M., Deslandes, L., Berthomé, R. et al. (2020) A complex network of additive and epistatic quantitative trait loci underlies natural variation of *Arabidopsis thaliana* quantitative disease resistance to *Ralstonia solanacearum* under heat stress. *Molecular Plant Pathology*, 21, 1405–1420.

Aoun, N., Tauleigne, L., Lonjon, F., Deslandes, L., Vailleau, F., Roux, F. et al. (2017) Quantitative disease resistance under elevated temperature: genetic basis of new resistance mechanisms to *Ralstonia solanacearum*. *Frontiers in Plant Science*, 8, 1387.

Atwell, S., Huang, Y.S., Vilhjálmsson, B.J., Willems, G., Horton, M., Li, Y. et al. (2010) Genome-wide association study of 107 phenotypes in *Arabidopsis thaliana* inbred lines. *Nature*, 465, 627–631.

Badet, T., Léger, O., Barascud, M., Voisin, D., Sadon, P., Vincent, R. et al. (2019) Expression polymorphism at the *ARPC4* locus links the actin cytoskeleton with quantitative disease resistance to *Sclerotinia sclerotiorum* in *Arabidopsis thaliana*. *New Phytologist*, 222, 480–496.

Bartoli, C. & Roux, F. (2017) Genome-wide association studies in plant pathosystems: toward an ecological genomics approach. *Frontiers in Plant Science*, 8, 763.

Bergelson, J. & Roux, F. (2010) Towards identifying genes underlying ecologically relevant traits in *Arabidopsis thaliana*. *Nature Reviews Genetics*, 11, 867–879.

Bernsdorff, F., Döring, A.-C., Gruner, K., Schuck, S., Bräutigam, A. & Zeier, J. (2016) Pipecolic acid orchestrates plant systemic acquired resistance and defense priming via salicylic acid-dependent and -independent pathways. *The Plant Cell*, 28, 102–129.

Bigeard, J., Colcombet, J. & Hirt, H. (2015) Signaling mechanisms in pattern-triggered immunity (PTI). *Molecular Plant*, 8, 521–539.

Bonhomme, M., Fariello, M.I., Navier, H., Hajri, A., Badis, Y., Miteul, H. et al. (2019) A local score approach improves GWAS resolution and detects minor QTL: application to *Medicago truncatula* quantitative disease resistance to multiple *Aphanomyces euteiches* isolates. *Heredity*, 123, 517–531.

Brachi, B., Faure, N., Horton, M., Flahauw, E., Vazquez, A., Nordborg, M. et al. (2010) Linkage and association mapping of *Arabidopsis thaliana* flowering time in nature. *PLoS Genetics*, 6, e1000940.

Brachi, B., Villoutreix, R., Faure, N., Hautekèete, N., Piquot, Y., Pauwels, M. et al. (2013) Investigation of the geographical scale of adaptive phenological variation and its underlying genetics in *Arabidopsis thaliana*. *Molecular Ecology*, 22, 4222–4240.

Büttner, D. (2012) Protein export according to schedule: architecture, assembly, and regulation of type III secretion systems from plant- and animal-pathogenic bacteria. *Microbiology and Molecular Biology Reviews*, 76, 262–310.

Cesari, S. (2018) Multiple strategies for pathogen perception by plant immune receptors. *New Phytologist*, 219, 17–24.

Chen, J.-G. (2006) RACK1 mediates multiple hormone responsiveness and developmental processes in *Arabidopsis*. *Journal of Experimental Botany*, 57, 2697–2708.

Cheng, Z., Li, J.-F., Niu, Y., Zhang, X.-C., Woody, O.Z., Xiong, Y. et al. (2015) Pathogen-secreted proteases activate a novel plant immune pathway. *Nature*, 521, 213–216.

Coll, N.S. & Valls, M. (2013) Current knowledge on the *Ralstonia solanacearum* type III secretion system. *Microbial Biotechnology*, 6, 614–620.

Cunnac, S., Occhialini, A., Barberis, P., Boucher, C. & Genin, S. (2004) Inventory and functional analysis of the large Hrp regulon in *Ralstonia solanacearum*: identification of novel effector proteins translocated to plant host cells through the type III secretion system. *Molecular Microbiology*, 53, 115–128.

Debieu, M., Huard-Chauveau, C., Genissel, A., Roux, F. & Roby, D. (2016) Quantitative disease resistance to the bacterial pathogen *Xanthomonas campestris* involves an *Arabidopsis* immune receptor pair and a gene of unknown function. *Molecular Plant Pathology*, 17, 510–520.

Deslandes, L., Olivier, J., Peeters, N., Feng, D.X., Khounlotham, M., Boucher, C. et al. (2003) Physical interaction between RRS1-R, a protein conferring resistance to bacterial wilt, and PopP2, a type III effector targeted to the plant nucleus. *Proceedings of the National Academy of Sciences USA*, 100, 8024–8029.

Deslandes, L., Olivier, J., Theulieres, F., Hirsch, J., Feng, D.X., Bittner-Eddy, P. et al. (2002) Resistance to *Ralstonia solanacearum* in *Arabidopsis thaliana* is conferred by the recessive *RRS1-R* gene, a member of a novel family of resistance genes. *Proceedings of the National Academy of Sciences USA*, 99, 2404–2409.

Deslandes, L., Pileur, F., Liaubet, L., Camut, S., Can, C., Williams, K. et al. (1998) Genetic characterization of *RRS1*, a recessive locus in *Arabidopsis thaliana* that confers resistance to the bacterial soil-borne pathogen *Ralstonia solanacearum*. *Molecular Plant-Microbe Interactions*, 11, 659–667.

Dinolfo, M.I., Castañares, E. & Stenglein, S.A. (2017) Resistance of *Fusarium poae* in *Arabidopsis* leaves requires mainly functional JA and ET signaling pathways. *Fungal Biology*, 121, 841–848.

Ebeed, H.T., Stevenson, S.R., Cuming, A.C. & Baker, A. (2018) Conserved and differential transcriptional responses of peroxisome associated pathways to drought, dehydration and ABA. *Journal of Experimental Botany*, 69, 4971–4985.

Frachon, L., Bartoli, C., Carrère, S., Bouchez, O., Chaubet, A., Gautier, M. et al. (2018) A genomic map of climate adaptation in *Arabidopsis thaliana* at a micro-geographic scale. *Frontiers in Plant Science*, 9, 967.

Frachon, L., Libourel, C., Villoutreix, R., Carrère, S., Glorieux, C., Huard-Chauveau, C. et al. (2017) Intermediate degrees of synergistic pleiotropy drive adaptive evolution in ecological time. *Nature Ecology & Evolution*, 1, 1551–1561.

Frachon, L., Mayjonade, B., Bartoli, C., Hautekèete, N.C. & Roux, F. (2019) Adaptation to plant communities across the genome of *Arabidopsis thaliana*. *Molecular Biology & Evolution*, 36, 1442–1456.

French, E., Kim, B.-S. & Iyer-Pascuzzi, A.S. (2016) Mechanisms of quantitative disease resistance in plants. *Seminars in Cell & Developmental Biology*, 56, 201–208.

Gallais, A. (1990) Quantitative genetics of doubled haploid populations and application to the theory of line development. *Genetics*, 124, 199–206.

Godiard, L., Sauviac, L., Torii, K.U., Grenon, O., Mangin, B., Grimsley, N.H. et al. (2003) ERECTA, an LRR receptor-like kinase protein controlling development pleiotropically affects resistance to bacterial wilt. *The Plant Journal*, 36, 353–365.

Guo, J., Wang, J., Xi, L., Huang, W.-D., Liang, J. & Chen, J.-G. (2009) RACK1 is a negative regulator of ABA responses in *Arabidopsis*. *Journal of Experimental Botany*, 60, 3819–3833.

Hayward, A.C. (1991) Biology and epidemiology of bacterial wilt caused by *Pseudomonas solanacearum*. *Annual Review of Phytopathology*, 29, 65–87.

Hernández-Blanco, C., Feng, D.X., Hu, J., Sánchez-Vallet, A., Deslandes, L., Llorente, F. et al. (2007) Impairment of cellulose synthases required for *Arabidopsis* secondary cell wall formation enhances disease resistance. *The Plant Cell*, 19, 890–903.

Hirsch, J., Deslandes, L., Feng, D.X., Balagué, C. & Marco, Y. (2002) Delayed symptom development in *ein2-1*, an *Arabidopsis* ethylene-insensitive mutant, in response to bacterial wilt caused by *Ralstonia solanacearum*. *Phytopathology*, 92, 1142–1148.

Horton, M.W., Hancock, A.M., Huang, Y.S., Toomajian, C., Atwell, S., Auton, A. et al. (2012) Genome-wide patterns of genetic variation in worldwide *Arabidopsis thaliana* accessions from the RegMap panel. *Nature Genetics*, 44, 212–216.

ten Hove, C.A., Bochdanovits, Z., Jansweijer, V.M.A., Koning, F.G., Berke, L., Sanchez-Perez, G.F. et al. (2011) Probing the roles of *LRR RLK* genes in *Arabidopsis thaliana* roots using a custom T-DNA insertion set. *Plant Molecular Biology*, 76, 69–83.

Huard-Chauveau, C., Perchepied, L., Debieu, M., Rivas, S., Kroj, T., Kars, I. et al. (2013) An atypical kinase under balancing selection confers broad-spectrum disease resistance in *Arabidopsis*. *PLoS Genetics*, 9, e1003766.

Huet, G. (2014) Breeding for resistances to *Ralstonia solanacearum*. *Frontiers in Plant Science*, 5, 715.

Iakovidis, M., Teixeira, P.J.P.L., Exposito-Alonso, M., Cowper, M.G., Law, T.F., Liu, Q. et al. (2016) Effector-triggered immune response in *Arabidopsis thaliana* is a quantitative trait. *Genetics*, 204, 337–353.

Islas-Flores, T., Rahman, A., Ullah, H. & Villanueva, M.A. (2015) The receptor for activated C kinase in plant signaling: tale of a promiscuous little molecule. *Frontiers in Plant Science*, 6, 1090.

Jia, X., Qin, H., Bose, S.K., Liu, T., He, J., Xie, S. et al. (2020) Proteomics analysis reveals the defense priming effect of chitosan oligosaccharides in *Arabidopsis*-Pst DC3000 interaction. *Plant Physiology and Biochemistry*, 149, 301–312.

Jones, J.D.G. & Dangl, J.L. (2006) The plant immune system. *Nature*, 444, 323–329.

Kang, H.M., Sul, J.H., Service, S.K., Zaitlen, N.A., Kong, S.-Y., Freimer, N.B. et al. (2010) Variance component model to account for sample structure in genome-wide association studies. *Nature Genetics*, 42, 348–354.

Karasov, T.L., Kniskern, J.M., Gao, L., DeYoung, B.J., Ding, J., Dubiella, U. et al. (2014) The long-term maintenance of a resistance polymorphism through diffuse interactions. *Nature*, 512, 436–440.

Kazan, K. & Manners, J.M. (2013) MYC2: the master in action. *Molecular Plant*, 6, 686–703.

Kim, S., Plagnol, V., Hu, T.T., Toomajian, C., Clark, R.M., Ossowski, S. et al. (2007) Recombination and linkage disequilibrium in *Arabidopsis thaliana*. *Nature Genetics*, 39, 1151–1155.

Landry, D., González-Fuente, M., Deslandes, L. & Peeters, N. (2020) The large, diverse, and robust arsenal of *Ralstonia solanacearum* type III effectors and their in planta functions. *Molecular Plant Pathology*, 21, 1377–1388.

Le Roux, C., Huet, G., Jauneau, A., Camborde, L., Trémousaygue, D., Kraut, A. et al. (2015) A receptor pair with an integrated decoy converts pathogen disabling of transcription factors to immunity. *Cell*, 161, 1074–1088.

Li, J., Bi, F.-C., Yin, J., Wu, J.-X., Rong, C., Wu, J.-L. et al. (2015) An *Arabidopsis* neutral ceramidase mutant *ncer1* accumulates hydroxy-ceramides and is sensitive to oxidative stress. *Frontiers in Plant Science*, 6, 460.

Liu, S., Kracher, B., Ziegler, J., Birkenbihl, R.P. & Somssich, I.E. (2015) Negative regulation of ABA signaling by WRKY33 is critical for *Arabidopsis* immunity towards *Botrytis cinerea* 2100. *eLife*, 4, e07295.

Lohou, D., Lonjon, F., Genin, S. & Vailleau, F. (2013) Type III chaperones & Co in bacterial plant pathogens: a set of specialized bodyguards mediating effector delivery. *Frontiers in Plant Science*, 4, 435.

Lohou, D., Turner, M., Lonjon, F., Cazalé, A.-C., Peeters, N., Genin, S. et al. (2014) HpaP modulates type III effector secretion in *Ralstonia solanacearum* and harbours a substrate specificity switch domain essential for virulence. *Molecular Plant Pathology*, 15, 601–614.

Lonjon, F., Lohou, D., Cazalé, A.-C., Büttner, D., Ribeiro, B.G., Péanne, C. et al. (2017) HpaB-dependent secretion of type III effectors in the plant pathogens *Ralstonia solanacearum* and *Xanthomonas campestris* pv. *vesicatoria*. *Scientific Reports*, 7, 4879.

Lonjon, F., Rengel, D., Roux, F., Henry, C., Turner, M., Le Ru, A. et al. (2020) HpaP sequesters HrpJ, an essential component of *Ralstonia solanacearum* virulence that triggers necrosis in *Arabidopsis*. *Molecular Plant-Microbe Interactions*, 33, 200–211.

Lonjon, F., Turner, M., Henry, C., Rengel, D., Lohou, D., van de Kerkhove, Q. et al. (2016) Comparative secretome analysis of *Ralstonia solanacearum* type 3 secretion-associated mutants reveals a fine control of effector delivery, essential for bacterial pathogenicity. *Molecular & Cellular Proteomics*, 15, 598–613.

Lopez-Huertas, E., Charlton, W.L., Johnson, B., Graham, I.A. & Baker, A. (2000) Stress induces peroxisome biogenesis genes. *The EMBO Journal*, 19, 6770–6777.

Lorang, J., Kidarsa, T., Bradford, C.S., Gilbert, B., Curtis, M., Tzeng, S.-C. et al. (2012) Tricking the guard: exploiting plant defense for disease susceptibility. *Science*, 338, 659–662.

Maekawa, T., Kracher, B., Vernaldi, S., Loren, V., van Themaat, E. & Schulze-Lefert, P. (2012) Conservation of NLR-triggered immunity across plant lineages. *Proceedings of the National Academy of Sciences USA*, 109, 20119–20123.

Marshall, A., Aalen, R.B., Audenaert, D., Beeckman, T., Broadley, M.R., Butenko, M.A. et al. (2012) Tackling drought stress: receptor-like kinases present new approaches. *The Plant Cell*, 24, 2262–2278.

Mayjonade, B., Gouzy, J., Donnadieu, C., Pouilly, N., Marande, W., Callot, C. et al. (2016) Extraction of high-molecular-weight genomic DNA for long-read sequencing of single molecules. *BioTechniques*, 61, 203–205.

Morel, A., Peeters, N., Vailleau, F., Barberis, P., Jiang, G., Berthomé, R. et al. (2018) Plant pathogenicity phenotyping of *Ralstonia solanacearum* strains. *Methods in Molecular Biology*, 1734, 223–239.

Peeters, N., Guidot, A., Vailleau, F. & Valls, M. (2013) *Ralstonia solanacearum*, a widespread bacterial plant pathogen in the post-genomic era. *Molecular Plant Pathology*, 14, 651–662.

Platt, A., Horton, M., Huang, Y.S., Li, Y., Anastasio, A.E., Mulyati, N.W. et al. (2010) The scale of population structure in *Arabidopsis thaliana*. *PLoS Genetics*, 6, e1000843.

R Studio Team. (2020) *RStudio: integrated development environment for R*. Boston, MA: RStudio.

Rajarammohan, S., Pradhan, A.K., Pental, D. & Kaur, J. (2018) Genome-wide association mapping in *Arabidopsis* identifies novel genes underlying quantitative disease resistance to *Alternaria brassicae*. *Molecular Plant Pathology*, 19, 1719–1732.

Roux, F., Noël, L., Rivas, S. & Roby, D. (2014) ZRK atypical kinases: emerging signaling components of plant immunity. *New Phytologist*, 203, 713–716.

Sabbagh, C.R.R., Carrere, S., Lonjon, F., Vailleau, F., Macho, A.P., Genin, S. et al. (2019) Pangenomic type III effector database of the plant pathogenic *Ralstonia* spp. *PeerJ*, 7, e7346.

van Schie, C.C.N. & Takken, F.L.W. (2014) Susceptibility genes 101: how to be a good host. *Annual Review of Phytopathology*, 52, 551–581.

Tarutani, Y., Morimoto, T., Sasaki, A., Yasuda, M., Nakashita, H., Yoshida, S. et al. (2004) Molecular characterization of two highly homologous receptor-like kinase genes, *RLK902* and *RKL1*, in *Arabidopsis thaliana*. *Bioscience, Biotechnology, and Biochemistry*, 68, 1935–1941.

Torii, K.U., Mitsukawa, N., Oosumi, T., Matsuura, Y., Yokoyama, R., Whittier, R.F. et al. (1996) The *Arabidopsis ERECTA* gene encodes a putative receptor protein kinase with extracellular leucine-rich repeats. *The Plant Cell*, 8, 735–746.

Wang, W., Wang, X., Wang, X., Ahmed, S., Hussain, S., Zhang, N.A. et al. (2019) Integration of RACK1 and ethylene signaling regulates plant growth and development in *Arabidopsis*. *Plant Science*, 280, 31–40.

Wu, G., Liu, S., Zhao, Y., Wang, W., Kong, Z. & Tang, D. (2015) ENHANCED DISEASE RESISTANCE4 associates with CLATHRIN HEAVY CHAIN2 and modulates plant immunity by regulating relocation of EDR1 in *Arabidopsis*. *The Plant Cell*, 27, 857–873.

Yue, X., Guo, Z., Shi, T., Song, L. & Cheng, Y. (2019) *Arabidopsis* AGC protein kinases IREH1 and IRE3 control root skewing. *Journal of Genetics and Genomics*, 46, 259–267.

Zaidi, S.-S.-E.-A., Mukhtar, M.S. & Mansoor, S. (2018) Genome editing: targeting susceptibility genes for plant disease resistance. *Trends in Biotechnology*, 36, 898–906.

Zhao, Y., Wu, G., Shi, H. & Tang, D. (2019) RECEPTOR-LIKE KINASE 902 associates with and phosphorylates BRASSINOSTEROID-SIGNALING KINASE1 to regulate plant immunity. *Molecular Plant*, 12, 59–70.

SUPPORTING INFORMATION

Additional Supporting Information may be found online in the Supporting Information section.